A NOVEL DESIGN TO REDUCE LOSSES AT DIELECTRIC WAVEGUIDE DISCONTINUITIES

El-Badawy El-Sharawy and Panayiotis A. Tirkas

Department of Electrical Engineering, Telecommunications Research Center
Arizona State University, Tempe, AZ 85287-7206

ABSTRACT

A novel approach to reduce losses of dielectric waveguide bends and junctions is examined in this paper. Ceramic material is added at the bend or the junction. The ceramic's dielectric constant, its shape and size, and position relative to the bend, are several parameters that can be varied to minimize the losses at the junction. Finite-difference time-domain analysis of a representative case is presented.

INTRODUCTION

The need for high-performance, higher bandwidth, communication systems has led to the development of technologies utilizing the millimeter-wave region. The millimeter-wave monolithic technology requires extensive use of planar conductors to realize various functions such as loads, transitions, junctions, and lines [1]. While this technology provides well-established processes with small tolerances in the fabrication of the circuit layouts, the conductor losses, substrate effects, and radiation losses degrade the performance considerably, resulting in lower device gain and signal-to-noise ratio [1].

Rectangular dielectric waveguides and their variants such as image guide, insular guide, trapped image line and suspended dielectric line are well suited for use in the millimeter-wave region [2]. Their low loss gives them an advantage over microstrip line and they are easier and less expensive to fabricate than metal waveguides [2]. Using dielectric components with minimal metallization becomes a necessity for high performance in this frequency region.

To achieve practical breakthrough using dielectric waveguides it is necessary to attain surface-mountable components and incorporate them into printed circuit boards. Ways to achieve dielectric waveguide transition into stripline and also the possibility of realizing circuit components such as dielectric resonators and filters are examined in [3]. The availability of high quality dielectric materials with high permittivity and resonance factor have made dielectric components suitable for applications in communications and broadcasting in the UHF band [3]. If dielectrics of still higher permittivity become available using new ceramic materials, the applicable frequency range may go down to as low as the VHF band.

Although dielectric waveguides are very useful for UHF applications, millimeter-wave applications, and optical-wave applications, they are very lossy at bends and junctions. To reduce the losses associated with the bends or junctions, a novel approach is examined by designing and embedding a high dielectric material at the position of the bend or junction. In this paper, finite-difference time-domain (FDTD) analysis of a dielectric waveguide bend demonstrates the effectiveness of this design. The finite-difference time-domain method has been used in the past by the authors in antenna analysis [4], [5] and electronic packaging [6], [7].

DIELECTRIC WAVEGUIDE BEND

An example of a dielectric waveguide bend is illustrated in Figure 1. The guidance principle employed in the dielectric waveguide is total reflection at the dielectric surfaces, which confines the transmitted energy to the interior of the dielectric waveguide. However, at a bend or junction, as the one illustrated in Figure 1, most of the energy is lost at the bend and does not make it to the output port. To reduce losses a high dielectric material is inserted at the bend. The dielectric constant, size, shape, relative position of the high dielectric material and shape of the dielectric waveguide bend, are some of the parameters that can be varied to minimize the losses.

The principle behind this design approach is to minimize the reflection coefficient as the wave impinges upon the high dielectric material, so as to reduce the reflected wave returning to the input port; minimize the transmission in the forward direction, so as to minimize the energy lost at the junction; and finally, to maximize the transmission in the direction of the bend so as to maximize the energy at the output port. These principles result in an optimum design. Simple transmission line methods were used in the design process to preselect the dielectric permittivity of the ceramic, and its position relative to the dielectric waveguide bend. The finite-difference time-domain method was

CH3577-4/95/0000-0841$01.00 © 1995 IEEE

then applied to analyze the structure obtained based on the simple transmission line approach.

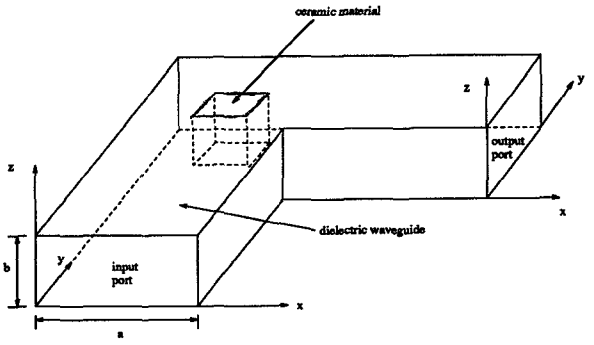

Figure 1: Dielectric waveguide juntion with ceramic material at the junction.

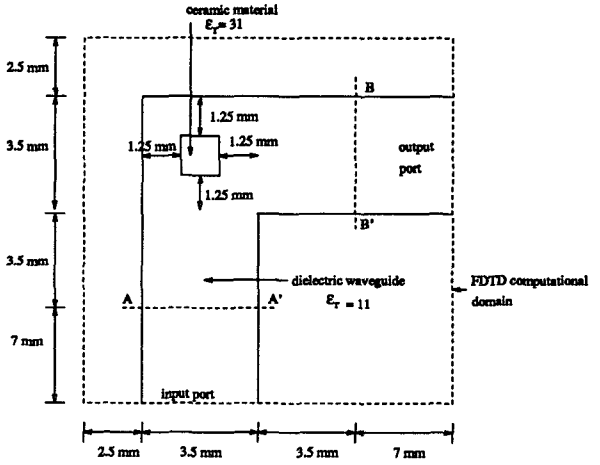

Figure 2: Top side of the dielectric waveguide bend with the presence of a ceramic piece and dimensions used for the analysis.

FDTD ANALYSIS AND RESULTS

Finite-difference time-domain analysis of the structure illustrated in Figure 1 was conducted with and without the high dielectric material at the position of the bend. The results from the two cases are presented and compared. For this analysis a dielectric waveguide of relative dielectric permittivity, $\epsilon_r = 11$ (Si), was used. The dimensions of the dielectric waveguide were $a = 3.5$ mm and $b = 2.5$ mm. The high dielectric material used was 1mm $\times$ 1mm $\times$ 2.5mm, with a relative dielectric permittivity, $\epsilon_r = 31$ (ceramic). The ceramic was positioned 1.25 mm from each side of the bend. The top view of the problem analyzed along with the relevant dimensions are shown in Figure 2. Using these dimensions, the estimated cutoff frequency of the dielectric waveguide was around 18 GHz.

At the input port, the excitation pulse used had the spatial distribution of the dominant TE_{10} mode used in rectangular metallic waveguides. The E_z component of the electric field was used at the input port to excite the dielectric waveguide. The expression used was:

$$E_z(x, y, z, t) = \sin(\frac{\pi}{a}x)\sin(2\pi f_c t) \qquad (1)$$

where $0 \leq x \leq a$, $0 \leq z \leq b$ and $y = 0$. The center frequency of the sinusoidal excitation was $f_c = 25$ GHz. The time step $\Delta t = \Delta x/2c$ in the FDTD formulation, where c is the speed of light in free space and $\Delta x = \Delta y = \Delta z = 0.25$ mm. To reach a steady state solution eight cycles of the wave were allowed. The required FDTD grid size was $32 \times 67 \times 67$ and the simulations were performed on an IBM RISC workstation. For the results presented in this paper first order Mur absorbing boundary conditions were used [8]. The accuracy of the simulations is expected to improve using the recently introduced Berenger perfectly matched layer absorbing boundary conditions [9]. Progress on the improved accuracy from the absorbing boundary conditions will be reported at the conference.

In Figures 3 and 4 the E_z amplitude distribution over the waveguide cross section at planes $A-A'$ and $B-B'$, respectively, without the presence of the high dielectric ceramic are illustrated. The amplitude distribution of E_z in the input side is shifted to the right (see Figure 3), whereas that of the output port is split into two high intensity regions (see Figure 4). This indicates the energy leakage outside the dielectric waveguide. In Figures 5 and 6 the E_z distribution over the same planes, with the presence of the ceramic material at the discontinuity are illustrated. In this case the amplitude distribution of E_z both at the input and output side is confined and almost symmetric within the dielectric waveguide cross section.

Since Maxwell's equations are solved in their finite-difference form, the dielectric waveguide modes would be generated based on the input excitation. At plane $A - A'$, the energy of the propagated pulse is obtained based on the excited modes and then integrated over the waveguide cross section to obtain the total input power to the dielectric waveguide. In a similar way, the output energy is found at plane $B - B'$ and then integrated over the cross section of the dielectric waveguide to obtain the power delivered to the output port.

Since the excitation was in time, the resulting electric and magnetic fields are also functions of time. The electric and magnetic field components along the dielectric waveguide cross section were converted to frequency domain by calculating their amplitude and relative phase, which are

then used to estimate the total power at the input port and transmitted power at the output port. A reference input power calculation was performed based on a straight dielectric waveguide section. From the input, reflected and transmitted power information, the insertion loss and return loss of the dielectric waveguide bend was obtained at 25 GHz. Based on the power calculations at 25 GHz, the return loss of the dielectric waveguide bend without the ceramic was $s_{11} = -10.68$ dB and the insertion loss $s_{21} = -7.06$ dB. With the presence of the ceramic, the return loss was $s_{11} = -17.52$ dB and the insertion loss $s_{21} = -4.75$ dB.

CONCLUSIONS

It was found in this paper that the presence of a ceramic material at a dielectric waveguide discontinuity reduces the losses due to the bend and helps focus the propagating fields within the dielectric waveguide. The single frequency analysis based on the FDTD method was extended to obtain broadband s-parameter results for the dielectric waveguide bend with and without the presence of the ceramic. The results from this analysis will be presented at the conference.

REFERENCES

[1] L. P. B. Katehi, "Novel Transmission Lines for the Submillimeter-Wave Region," *Proc. IEEE*, Vol. 80, pp. 1771-1787, Nov. 1992.

[2] J. W. Mink and F. K. Schwering, "A hybrid Dielectric Slab-Beam Waveguide for the Sub-Millimeter Wave Region," *IEEE Trans. Microwave Theory Tech.*, Vol. 41, pp. 1720-1729, Oct. 1993.

[3] Y. Konishi, "Novel Dielectric Waveguide Components - Microwave Applications of New Ceramic Materials," *Proc. IEEE*, Vol. 74, pp. 726-740, June 1991.

[4] P.A. Tirkas, C.A. Balanis, M.P. Purchine, G.C. Barber, "Finite-Difference Time-Domain Method for Antenna Radiation, Interference, and Interaction With Complex Structures," in *IEEE Trans. Electromag. Compat.*, Vol. 35, pp. 192-203, May 1993

[5] P.A. Tirkas, C.A. Balanis and R.A. Renaut, "Higher Order Absorbing Boundary Conditions for the Finite-Difference Time-Domain Method," in *IEEE Trans. Antennas Propagat.*, Vol. 40, pp. 1215-1222, Oct. 1992.

[6] P.A. Tirkas, S. El-Ghazaly, S. Rajan, E. El-Sharawy, and C.A. Balanis, "Characterization of High Performance Packages: Electrical, Thermal, and Stress Issues," *1995 National Radio Science Meeting* (Boulder, CO), Jan. 3, 1995.

[7] P.A. Tirkas, S. El-Ghazaly, S. Rajan, E. El-Sharawy, and C.A. Balanis, "Electrical, Thermal, and Stress Analysis of Flip-Chip Electronic Packages," *PIERS 1995: Progress Electromag. Resrch Sympos.*, (Seattle, WA), Jul. 24, 1995, accepted.

[8] G. Mur, "Absorbing Boundary Conditions for the Finite-Difference Approximation of the Time-Domain Electromagnetic-Field Equations," *IEEE Trans. Electromag. Compat.*, Vol. 23, pp. 377-382, Nov. 1981.

[9] J. Berenger, "A Perfectly Matched Layer for the Absorption of Electromagnetic Waves," *J. Comput. Physics*, **114**, pp.185-200, 1994.

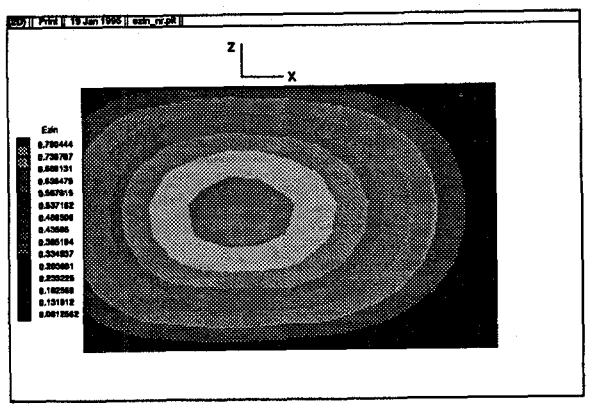

Figure 3: E_z amplitude distribution across the waveguide cross section in the input port, without the presence of the ceramic.

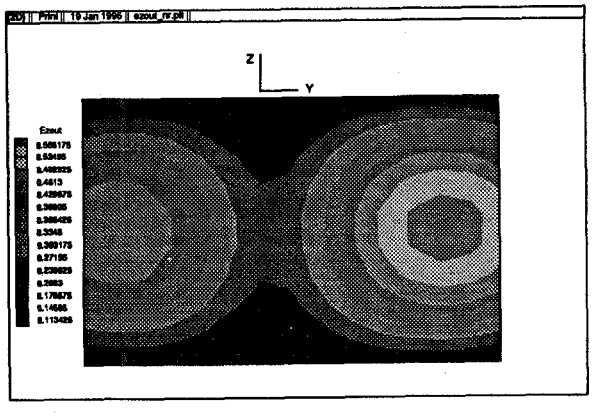

Figure 4: E_z amplitude distribution across the waveguide cross section in the output port, without the presence of the ceramic.

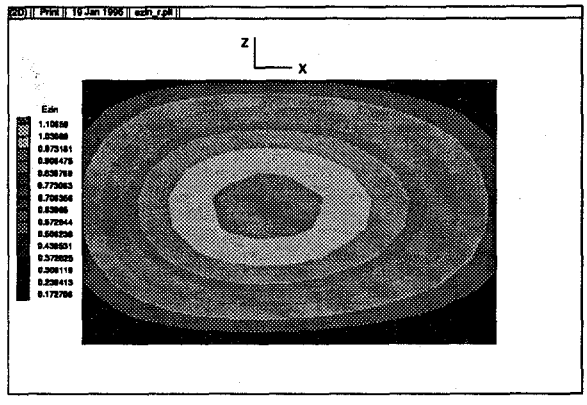

Figure 5: E_z amplitude distribution across the waveguide cross section in the input port, with the presence of the ceramic.

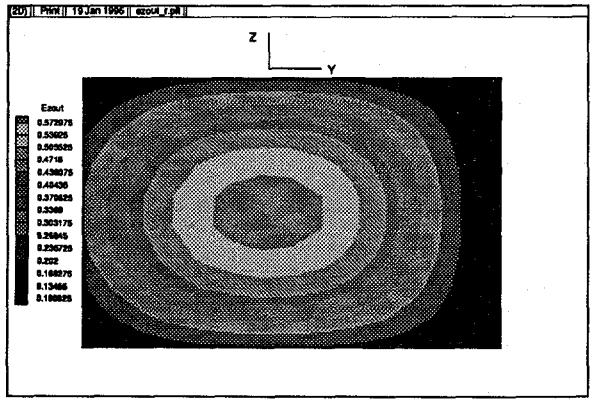

Figure 6: E_z amplitude distribution across the waveguide cross section in the output port, with the presence of the ceramic.